ARTICLE

Sorting nexin 3 induces heart failure via promoting retromer-dependent nuclear trafficking of STAT3

Jing Lu [1] · Suowen Xu[2,3] · Yuqing Huo[4] · Duanping Sun [5] · Yuehuai Hu[1] · Junjian Wang[1] · Xiaolei Zhang[1] · Panxia Wang[1] · Zhuoming Li[1] · Mengya Liang[6] · Zhongkai Wu[6] · Peiqing Liu[1]

Abstract

Sorting nexins (SNXs), the retromer-associated cargo binding proteins, have emerged as critical regulators of the trafficking of proteins involved in the pathogenesis of diverse diseases. However, studies of SNXs in the development of cardiovascular diseases, especially cardiac hypertrophy and heart failure, are lacking. Here, we ask whether SNX3, the simplest structured isoform in the SNXs family, may act as a key inducer of myocardial injury. An increased level of SNX3 was observed in failing hearts from human patients and mice. Cardiac-specific *Snx3* knockout (*Snx3-cKO*) mice and *Snx3* transgenic (*Snx3-cTg*) mice were generated to evaluate the role of *Snx3* in myocardial hypertrophy, fibrosis, and heart function by morphology, echocardiography, histological staining, and hypertrophic biomarkers. We report that *Snx3-cKO* in mice significantly protected against isoproterenol (ISO)-induced cardiac hypertrophy at 12 weeks. Conversely, *Snx3-cTg* mice were more susceptible to ISO-induced cardiac hypertrophy at 12 weeks and showed aggravated cardiac injury even heart failure at 24 weeks. Immunoprecipitation-based mass spectrometry, immunofluorescent staining, co-immunoprecipitation, localized surface plasmon resonance, and proximity ligation assay were performed to examine the direct interaction of SNX3-retromer with signal transducer and activator of transcription 3 (STAT3). We discovered that STAT3 was a new interacting partner of SNX3-retromer, and SNX3-retromer served as an essential platform for assembling gp130/JAK2/STAT3 complexes and subsequent phosphorylation of STAT3 by direct combination at EE. SNX3-retromer and STAT3 complexes were transiently imported into the nucleus after hypertrophic stimuli. The pharmacological inhibition or knockdown of STAT3 reversed SNX3 overexpression-induced myocardial injury. STAT3 overexpression blunts the beneficial function of SNX3 knockdown on hypertrophic cardiomyocytes. We show that SNX3-retromer promoted importin α3-mediated STAT3 nuclear trafficking and ultimately leading to cardiac injury. Taken together, our study reveals that SNX3 plays a key role in cardiac function and implicates SNX3 as a potential therapeutic target for cardiac hypertrophy and heart failure.

✉ Zhongkai Wu
wuzhk@mail.sysu.edu.cn

✉ Peiqing Liu
liupq@mail.sysu.edu.cn

1 School of Pharmaceutical Sciences, National and Local United Engineering Lab of Druggability and New Drugs Evaluation, Sun Yat-sen University, Guangzhou, P. R. China

2 Aab Cardiovascular Research Institute, University of Rochester School of Medicine and Dentistry, Rochester, NY, USA

3 Department of Endocrinology, the First Affiliated Hospital of USTC, Division of Life Sciences and Medicine, University of Science and Technology of China, Hefei, P. R. China

4 Department of Cellular Biology and Anatomy, Medical College of Georgia, Vascular Biology Center, Augusta University, Augusta, GA, USA

5 Center for Drug Research and Development, Guangdong Pharmaceutical University, Guangzhou, P.R. China

6 Department of Cardiac Surgery, First Affiliated Hospital, Sun Yat-sen University, Guangzhou, P.R. China

Introduction

By responding to various pathophysiological stresses, the heart undergoes a transition from compensatory hypertrophy

to decompensatory phase, in which left ventricular remodeling, systolic and diastolic dysfunction and eventual heart failure (HF) occurs [1–3]. The abnormal activation of multiple cellular signaling pathways, such as protein kinase C (PKC)-mitogen-activated protein kinase (MAPK), a calcineurin-nuclear factor of activated T cells (NFATs), and janus kinase (JAK)-signal transducer and activator of transcription protein (STAT), is the pathological basis for the development of HF [3, 4].

The physiological functions of signaling proteins are closely linked to their intracellular trafficking and subcellular localization, which is determined by sorting nexins (SNXs)–retromer complex and endosomes [5–8]. SNXs are featured by a highly conserved Phox homology (PX)-domain and comprise 33 members in mammals [9]. Structurally, SNXs directly or indirectly bind to vacuolar protein sorting (VPS) family, VPS26 VPS35 and VPS29, to constitute retromer complex; SNXs also target the endosomal membrane through the PX-domain [5, 6]. Functionally, SNXs recruit retromer to early endosomes (EE) or recycling endosomes (RE) and subsequently mediate retrograde transport of cargo proteins via vesicle budding from EE/RE to trans-Golgi network (TGN), plasma membrane (PM), or cell nucleus [5–7]. SNXs have been reported to regulate diverse disease processes, including Alzheimer's disease, cancer, HF, and arthritis [10–13]. For instance, we previously reported that deficiency of SNX10 prevents inflammation and bone erosion in a mouse model of rheumatoid arthritis through promoting NFATc1 degradation [10]; SNX13 profoundly affects cardiac performance through apoptosis repressor with caspase recruitment domain (ARC)-caspase signaling pathway [11]. Recently, it is found that SNX3 (the simplest structured isoform in the SNXs family)-retromer is required for retrograde recycling of Wntless [14], PC1, and PC2 [15], the cation-independent mannose 6-phosphate receptor (CI-M6PR) [16], and iron transporters [17]. However, the role of SNX3 in the pathogenesis of cardiovascular diseases, especially cardiac hypertrophy and HF, remains unknown.

Signal transducer and activator of transcription 3 (STAT3), a subtype of STAT family, participates in the pathological process of cardiac hypertrophy and HF [4, 18, 19]. Cardiomyocyte-specific overexpressed STAT3 (Stat3-Tg) in mice causes spontaneous concentric cardiac hypertrophy [4]. In response to stimulation with pro-inflammatory cytokines and growth factors, STAT3 is phosphorylated at tyrosine 705 (Y705) by receptor-associated JAK2, then forms homo- or hetero-dimers, and translocate to the cell nucleus where they act as transcription activators [18–20]. Importin α3 (also called Kpna3), a nuclear import factor, is responsible for STAT3 nuclear import independent of tyrosine phosphorylation [21, 22]. Upon axons injury exposure, the newly synthesized STAT3

combines with importin α5 and dynein (a retrograde molecular motor) and transports back to the cell body [23–25]. STAT3 co-localizes with endocytic vesicles in transit from the cell membrane to the perinuclear region, the perinuclear endosomal compartment to sustain phosphorylated STAT3 (Y705) in the nucleus [26–29]. To date, it remains largely unknown whether the retromer-dependent mechanism is involved in the phosphorylation and nuclear trafficking of STAT3.

Here, we demonstrate that the mRNA and protein levels of SNX3 were increased in end-stage failing human hearts and cardiac tissues from isoproterenol (ISO)-induced mouse cardiac injury model. Besides, cardiac-specific Snx3 knockout (Snx3-cKO) in mice efficaciously protected against ISO-induced cardiac injury at 12 weeks. Conversely, cardiac-specific Snx3 transgenic (Snx3-cTg) mice were hypersensitive to ISO-induced cardiac injury at 12 weeks and resulted in cardiac hypertrophy and dysfunction even HF at 24 weeks. Our results reveal the importance of the SNX3–retromer complex for assembling gp130/JAK2/STAT3 complexes and subsequent phosphorylation of STAT3 by direct combination at EE. Hypertrophic stimulation-induced nuclear translocation of STAT3 was facilitated by importin α3-mediated SNX3–retromer importing. The pharmacological inhibition or knockdown of STAT3 reversed SNX3 overexpression-induced myocardial injury. STAT3 overexpression blunts the beneficial function of SNX3 knockdown on hypertrophic cardiomyocytes. SNX3–retromer promoted STAT3 nuclear trafficking and ultimately leading to cardiac injury. Together, our study identifies SNX3 as a potential target for cardiac hypertrophy and HF.

Results

SNX3 expression was up-regulated in human and mouse failing hearts

To explore the potential role of SNX3 in the development of HF, we analyzed heart samples from 9 patients with HF in end-stage and 3 non-failing healthy controls. The SNX3 mRNA level was increased in failing human heart tissues compared with that in the normal control tissues as shown by qPCR (Supplementary Fig. S1). The results from immunofluorescence (IF) and western blot analysis suggest that the protein expression of SNX3 was significantly higher in the failing human heart tissues (Fig. 1A, B). Similarly, the mRNA and protein levels of SNX3 were clearly induced in the myocardium of mouse cardiac hypertrophy and HF model by subcutaneous (s.c.) injection of ISO (3 mg/kg/day, a classic hypertrophic agonist [30–32]) (Supplementary Fig. S2). These results suggest
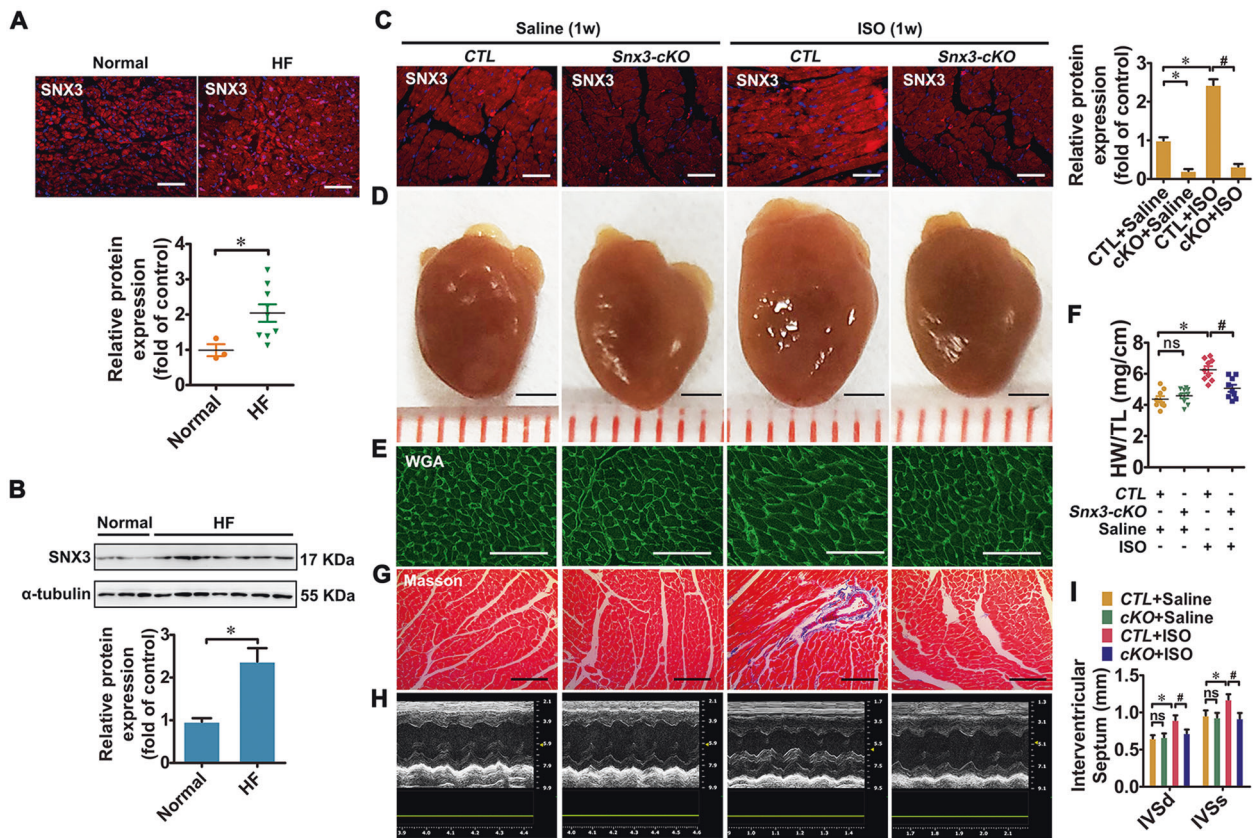
Fig. 1 SNX3 expression was increased in failing human hearts, and cardiac-specific *Snx3-cKO* mice were protected from ISO-induced cardiac injury. A and **B** A significant induction of SNX3 protein expression in end-stage failing human heart tissues ($n = 9$ per HF, $n = 3$ per normal control), which was identified by IF assay (Scale bar: 200 μm) and western blot analysis. Male C57BL/6 *Snx3-cKO* mice and their respective *CTL* at 11 weeks were injected with ISO (3 mg/kg/day, s.c.) or an equal volume of sterile normal saline for one week. **C** The protein expression of SNX3 was measured by an IF assay (Scale bar: 100 μm). **D** and **E** Gross observation of heart morphology, WGA staining (Scale bar: 50 μm)-stained cross-sections of heart tissues were shown. **F** The HW/TL ratio was calculated. **G** Masson staining (Scale bar: 100 μm)-stained cross-sections of heart tissues were shown. **H** The

representative echocardiographic graphs were presented. **I** The echocardiographic parameters IVS was measured. Representative images of five independent experiments were presented. The data were presented as the means ± SEM. *$P < 0.05$ vs. Normal or *CTL* + Saline group, #$P < 0.05$ vs. *CTL* + ISO group, $n = 11$ per *CTL* + Saline group, $n = 11$ per *cKO* + Saline group, $n = 10$ per *CTL* + ISO group, $n = 12$ per *cKO* + ISO group. *CTL* littermate negative control, HF heart failure, HW/TL, the heart weight to the tibia length ratio, IF immunofluorescence, ISO isoproterenol, IVS interventricular septum, ns no statistical difference, s.c. subcutaneously, *Snx3-cKO* cardiac-specific *Snx*3 knockout, WGA wheat germ agglutinin, 1w 1 week. See also Supplementary Figs. S1–S4.

that SNX3 was associated with cardiac hypertrophy and HF in humans and mice.

Cardiac-specific *Snx3-cKO* attenuated ISO-induced cardiac hypertrophy in mice

To examine the function of SNX3 in cardiac hypertrophy, a cardiac-specific *Snx3-cKO* mice model was generated by breeding *Snx3*-floxed mice with C57BL/6-*Myh6*$^{em1(IRES-Cre)Smoc}$ line (Supplementary Fig. S3A). A cDNA encoding internal ribosome entry site (IRES) and Cre recombinase is inserted into the 3′UTR region of α-myosin heavy chain (Myh6) gene to generate this Myh6-IRES-Cre mouse line [33]. As shown in Fig. 1C, Supplementary Fig. S3F and G, endogenous SNX3 protein expression was specifically depleted in heart tissues of

Snx3-cKO mice, compared with their littermate negative controls (*CTL*). *Snx3-cKO* mice showed no obvious cardiac structural or functional defects at basal conditions.

To assess whether *Snx3* deletion influences cardiac dysfunction under stressed conditions, at 11 weeks, both *Snx3-cKO* mice and *CTL* mice were randomly injected with ISO (3 mg/kg/day, s.c.) for one week to establish a cardiac hypertrophy model. Compared with the saline group, ISO treatment significantly induced cardiac hypertrophy, fibrosis, and heart dysfunction in *CTL* mice, evidenced by gross morphologic examination, histological staining, hypertrophic biomarkers (*Anf*, *Bnp,* and *β-Mhc*), heart weight to the tibia length ratio (HW/TL) and echocardiography (Fig. 1D–I, Supplementary Fig. S4). The results of heart morphology, wheat germ agglutinin (WGA) staining,

hematoxylin–eosin (HE) staining, HW/TL ratio, as well as the mRNA levels of hypertrophic biomarkers, demonstrated that ISO treatment-induced cardiomyocyte hypertrophy in *CTL* mice (Fig. 1D–F, Supplementary Fig. S4A, C). Cardiac fibrosis was exhibited by masson staining and picric sirius red (PSR) staining in *CTL* + ISO group (Fig. 1G, Supplementary Fig. S4B). The increase of cardiomyocyte size and cardiac fibrosis induced by ISO were significantly reduced in *Snx3-cKO* mice (Fig. 1D–G, Supplementary Fig. S4A–C). Data of echocardiography, such as ejection fraction (EF), fractional shortening (FS), cardiac output (CO), stroke volume (SV), left ventricular diameter (LVID), and left ventricular volume (LVV), were significantly reduced, while left ventricular mass (LVM), interventricular septum (IVS) and left ventricular posterior wall thickness (LVPW) were increased in ISO group, which was partially

recovered by *Snx3* knockout (Fig. 1I, Supplementary Fig. S4D–L). These results suggest that knockout of *Snx3* significantly alleviated ISO-induced cardiac injury and heart dysfunction in mice.

Cardiac-specific *Snx3* transgene led to HF in mice

To further determine whether SNX3 contributes to myocardial injury, cardiac-specific *Snx3-cTg* mice were generated by crossing *Snx3* transgenic mice with B6.FVB-Tg (Myh6-Cre)2182Mds/J mice (Fig. 2A, Supplementary Fig. S5). This transgenic strain uses a Cre/loxP approach in which transgenic Cre expression is driven by the mouse Myh6 promoter [34]. Compared with littermate negative controls (*N-Tg*), the expression of SNX3 protein is robustly expressed in the heart of *Snx3-cTg* mice, as indicated by
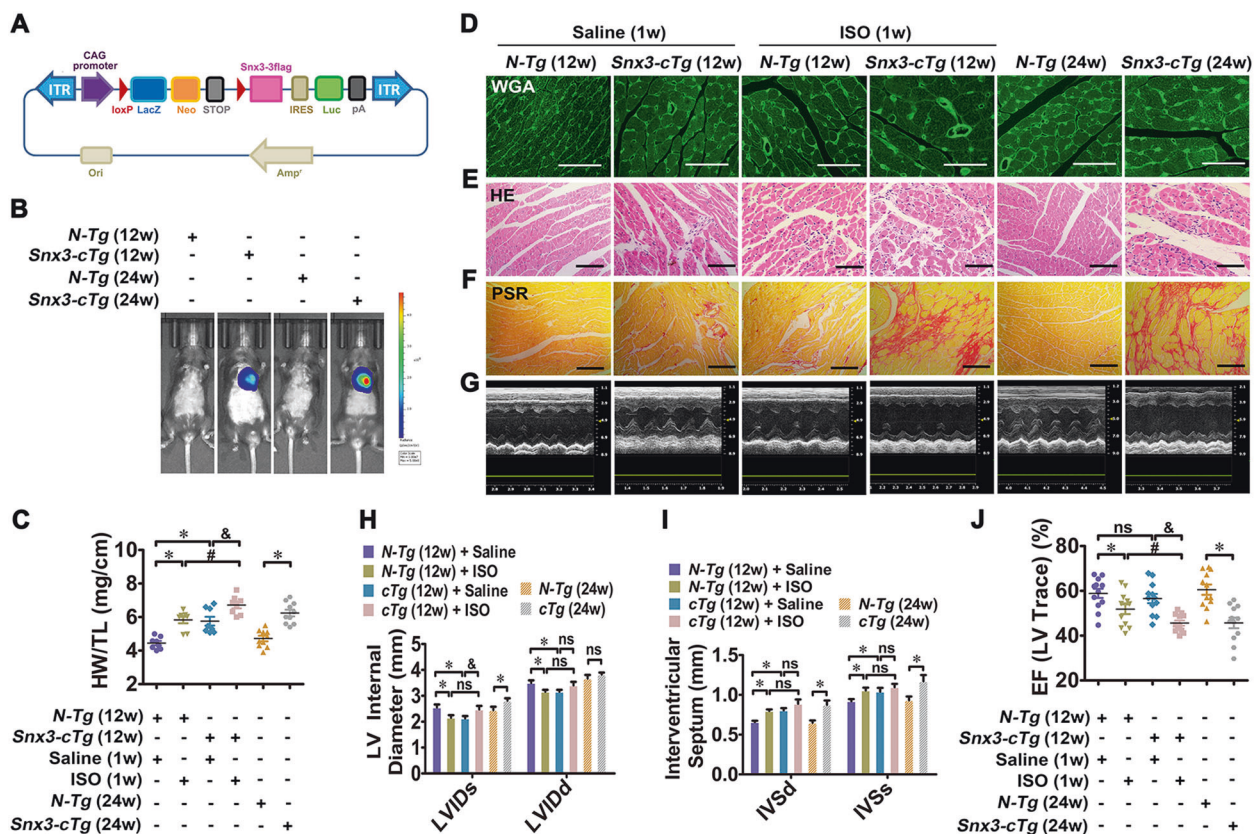

Fig. 2 Cardiac-specific *Snx3* transgene led to myocardial injury in mice. We investigated the changes in cardiac structure and function in *Snx3-cTg* mice at 12 and 24 weeks. Besides, *Snx3-cTg* mice (at 11 weeks) were injected with 3 mg/kg/d ISO (s.c.) or an equal volume of sterile normal saline for one week. **A** The scheme of *Snx3-cTg* mice construction strategy was shown. **B** The protein level of SNX3 was detected by live imaging. **C** The HW/TL ratio was calculated. **D–F** WGA staining (Scale bar: 50 μm), HE staining (Scale bar: 100 μm) and PSR staining (Scale bar: 100 μm)-stained cross-sections of heart tissues were shown. **G** The representative echocardiographic graphs were shown. **H–J** The echocardiographic parameters (LVID, IVS, and EF) were measured. Representative images of five independent experiments were presented. The data were shown as the

means ± SEM. *$P < 0.05$ vs. *N-Tg* (12w) + Saline or *N-Tg* (24w) group, #$P < 0.05$ vs. *N-Tg* (12w) + ISO group, &$P < 0.05$ vs. *Snx3-cTg* (12w) + Saline group. $n = 12$ per *N-Tg* (12w) + Saline group, $n = 11$ per *N-Tg* (12w) + ISO group, $n = 12$ per *Snx3-cTg* (12w) + Saline group, $n = 12$ per *Snx3-cTg* (12w) + ISO group, $n = 10$ per *N-Tg* (24w) group, $n = 9$ per *Snx3-cTg* (24w) group. EF ejection fraction, HE hematoxylin–eosin, HW/TL the heart weight to the tibia length ratio, ISO isoproterenol, IVS interventricular septum, LVID left ventricular diameter, ns no statistical difference, *N-Tg* non-transgenic, PSR picric sirius red, s.c. subcutaneously, *Snx3-cTg* cardiac-specific *Snx3* transgenic mice, WGA wheat germ agglutinin, 1w 1 week, 12w 12 weeks, 24w 24 weeks. See also Supplementary Figs. S5–S7.

western blot, IF assay, and the luciferase activity by live imaging (Fig. 2B, Supplementary Fig. S5E–H).

At 12 weeks of age, *Snx3-cTg* mice showed a mild degree of cardiac hypertrophy, as indicated by the following observations: (1) the larger heart/cardiac size by gross morphological examination, the increased hypertrophic biomarkers and HW/TL ratio, WGA staining, and HE staining (Fig. 2C–E, Supplementary Fig. S6A, B); (2) deposition of collagen protein by PSR staining (Fig. 2F); (3) echocardiography results (Fig. 2G) showed a decrease in LVID (Fig. 2H), CO (Supplementary Fig. S6C), SV (Supplementary Fig. S6D) and LVV (Supplementary Fig. S6F), as well as an increase in IVS (Fig. 2I), LVM (Supplementary Fig. S6E) and LVPW (Supplementary Fig. S6G). Overexpression of SNX3 did not apparently affect EF, FS, or heart rate (HR) in *Snx3-cTg* mice at 12 weeks (Fig. 2J, Supplementary Fig. S6H, I).

We also investigated whether overexpression of SNX3 aggravated ISO-induced cardiac hypertrophy in *Snx3-cTg* mice (12-weeks-old). There were signs of an increase in the cardiomyocyte size in both *N-Tg* mice and *Snx3-cTg* mice; however, *Snx3-cTg* mice have larger cardiomyocyte size than in *N-Tg* mice (Fig. 2C–E, Supplementary Fig. S6A, B). In addition, ISO-induced cardiac fibrosis was aggravated when SNX3 was overexpressed (Fig. 2F). After ISO infusion, severe heart dysfunction detected by echocardiography was noted in *Snx3-cTg* mice more than *N-Tg* mice (Fig. 2G–J, Supplementary Fig. S6C–I). These results suggest that *Snx3-cTg* mice were more susceptible to ISO-induced cardiac injury.

After 24 weeks, *Snx3-cTg* mice displayed significant hypertrophic growth of cardiomyocytes, increases in HW/TL ratios and hypertrophic biomarkers, myocardial fibrosis, compared with *N-Tg* mice (Fig. 2C–F, Supplementary Fig. S7A, B). According to the echocardiography (Fig. 2G), *Snx3-cTg* mice exhibited increases in LVID (Fig. 2H), IVS (Fig. 2I), LVM (Supplementary Fig. S7C), and LVV (Supplementary Fig. S7D), declines in EF (Fig. 2J), FS (Supplementary Fig. S7E), SV (Supplementary Fig. S7F) and CO (Supplementary Fig. S7G), implying that *Snx3-cTg* mice spontaneously developed severe heart dysfunction. These results suggest that the cardiac structure was disorganized and systole diastolic performances tend to be worsened with advancing age in *Snx3-cTg* mice.

SNX3-retromer directly interacted with STAT3 at EE

The prominent effects of SNX3 on cardiac hypertrophy and HF (Figs. 1 and 2, Supplementary Fig. S1–7) prompt us to investigate its underlying mechanisms. Since SNX3 is a key retromer-associated protein [5, 6], we thus examined whether retromer is involved in SNX3-mediated cardiac hypertrophy.

By immunoprecipitation-based mass spectrometry (IP-MS), we identified STAT3, as a new interacting partner of SNX3, in addition to known interacting proteins, such as retromer proteins VPS26 and VPS35 (Supplementary Fig. S8A, B). To validate the interaction of SNX3 and STAT3, neonatal rat cardiomyocytes (NRCMs) were infected with Ad-SNX3 (Flag-tagged) or Ad-STAT3 (HA-tagged). Protein interaction was evaluated by IF staining and co-IP assays (Fig. 3A–C). Indeed, IF staining results indicate that HA-labeled STAT3 and retromer proteins (SNX3, VPS26, and VPS35) were located in the same cellular compartments (Fig. 3A). The co-IP results suggest that SNX3–retromer interacted with STAT3 in NRCMs and mouse heart tissues (Fig. 3B, C, Supplementary Fig. S8C–E). According to localized surface plasmon resonance (LSPR) results, recombinant STAT3 protein (117–770aa) directly interacted with SNX3, VPS35, and VPS26 with a binding constant at 7.10e−7, 1.58e−8, 1.30e−8 M (KD values), respectively (Supplementary Fig. S8F–L). The interaction between truncated STAT3 protein (576–678aa) and SNX3–retromer was shown in Fig. 3D with a binding constant at 6.11e−8, 5.06e−8, 1.01e−7 M (KD values) in a cell-free system. Moreover, the proximity ligation assay (PLA) was performed to visually detect the protein–protein interactions using confocal microscopy. As shown in Supplementary Fig. S8M, the binding of SNX3 and STAT3 was located in the cytoplasm of normal cultured cardiomyocytes. However, the SNX3/STAT3 complex was induced by ISO treatment and was substantially localized in the nucleus (Supplementary Fig. S8M).

Besides, NRCMs were precipitated by anti-early endosome antigen 1 (EEA1), Rab5, and clathrin heavy chain (CHC) (markers of early endosome), SNX3 and STAT3 were found in the precipitation of EE by co-IP assays (Fig. 3E, Supplementary Fig. S9A and B). However, no significant binding of SNX3 and Rab7, a marker of late endosome (LE), was detected by co-IP assays (Supplementary Fig. S9C). This result is also consistent with the previous report that SNX3–retromer is predominantly localized on EE and has little presence on LE [5, 6]. The early endosome fraction was purified from NRCMs using density gradient centrifugation, and detected by western blot analysis (Fig. 3F). We observed that both STAT3 and SNX3 mainly associated with EE in NRCMs, though some STAT3 positive staining was presented in LE and lysosomes, as suggested by STAT3 combining with the endosomal compartment markers (EEA1, Rab5, Rab7, and CHC) and lysosome marker (Lamp-2) (Fig. 3B, C, E, F, Supplementary Fig. S9D, E). These results imply that STAT3 directly interacted with SNX3–retromer at the early endosome in cardiomyocytes.
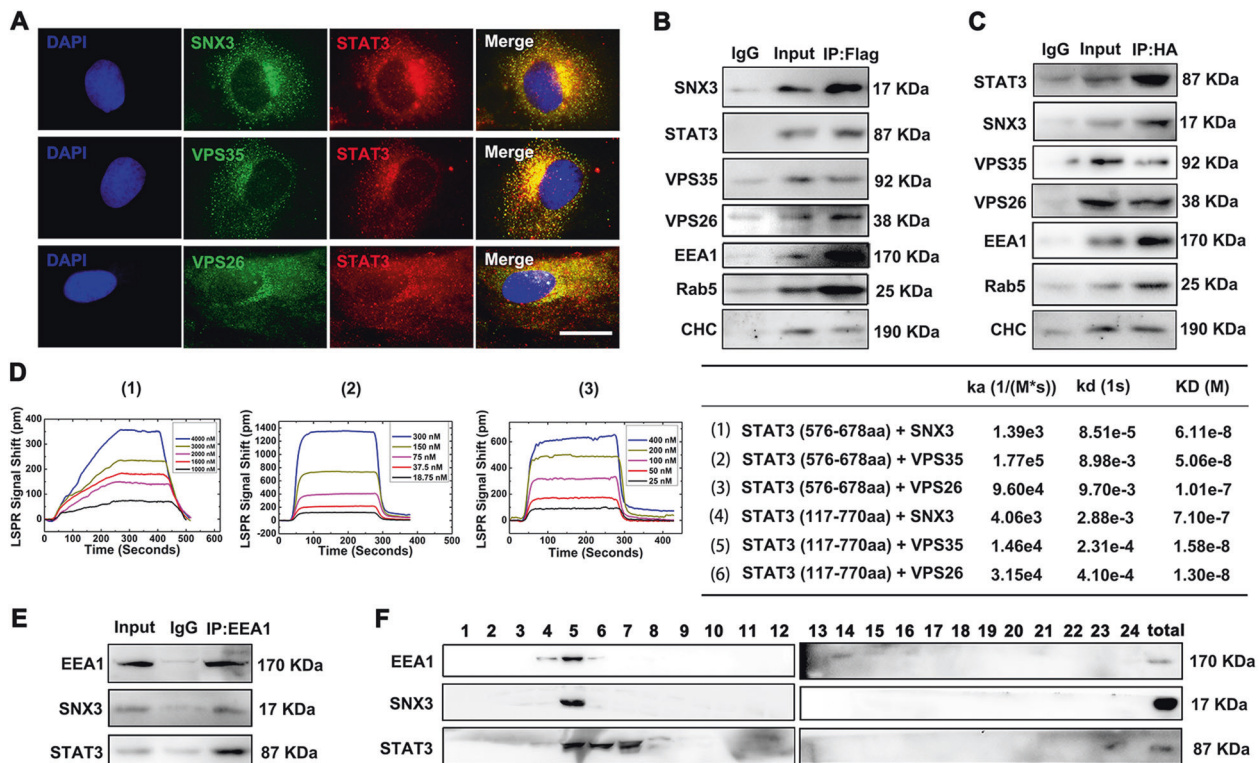
	ka (1/(M*s))	kd (1s)	KD (M)
(1) STAT3 (576-678aa) + SNX3	1.39e3	8.51e-5	6.11e-8
(2) STAT3 (576-678aa) + VPS35	1.77e5	8.98e-3	5.06e-8
(3) STAT3 (576-678aa) + VPS26	9.60e4	9.70e-3	1.01e-7
(4) STAT3 (117-770aa) + SNX3	4.06e3	2.88e-3	7.10e-7
(5) STAT3 (117-770aa) + VPS35	1.46e4	2.31e-4	1.58e-8
(6) STAT3 (117-770aa) + VPS26	3.15e4	4.10e-4	1.30e-8

Fig. 3 SNX3–retromer directly interacted with STAT3 at early endosomes in vivo and in vitro. A NRCMs were infected with Ad-STAT3 (HA-tagged) and were measured by IF staining using confocal microscopy (Scale bar: 25 µm). Representative images of five independent experiments were presented. NRCMs were infected with Ad-SNX3 (Flag-tagged) or Ad-STAT3 (HA-tagged) and were precipitated by anti-Flag (**B**) or anti-HA (**C**). **D** The binding curves of SNX3-retromer and truncated STAT3 protein (576-678aa) were measured by LSPR analysis, and the ka, kd, and KD values for STAT3 (576–678aa, 117–720aa), SNX3, VPS35, and VPS26 were calculated by Trace-Drawer™. **E** NRCMs were precipitated by anti-EEA1 (a marker for early endosome) for SNX3 and STAT3 detection in co-IP assays. **F** The early endosome fraction was purified from NRCMs using density gradient centrifugation, and detected by western blot. $n = 5$. CHC clathrin heavy chain; co-IP co-immunoprecipitation, IP–MS immunoprecipitation-based mass spectrometry, LSPR localized surface plasmon resonance, NRCMs neonatal rat cardiomyocytes. See also Supplementary Figs. S8 and S9.

SNX3–retromer served as a platform for STAT3 activation

It is well-established that JAK2/STAT3 pathway is involved in the pathogenesis of cardiac hypertrophy and HF [4]. To investigate whether SNX3 cooperates with STAT3 to mediate cardiac hypertrophy, we established three classical cardiac hypertrophic models (induced by ISO, angiotensin II (AngII), and phenylephrine (PE), respectively) in NRCMs (Fig. 4A, B). The phosphorylation levels of JAK2 (Y1007 and Y1008) and STAT3 (Y705), and the protein expression of SNX3 were enhanced in these hypertrophic models, whereas the protein levels of gp130 and STAT3 remained unchanged (Fig. 4C, Supplementary Fig. S10A). The homo-/hetero-dimerization of STAT3 and STAT1 was also increased by treatment with hypertrophy stimuli (Supplementary Fig. S10B).

Given that SNX3 is localized in retromer-containing endosomes [6], we investigated whether SNX3–retromer is involved in JAK2/STAT3 signaling. The results of co-IP and IF assays showed that ISO increased the association of STAT3 with SNX3, JAK2, and gp130, whereas knockdown of SNX3 decreased these interactions (Fig. 4D–F, Supplementary Fig. S11A). Consistently, knockdown of SNX3 significantly inhibited ISO-induced phosphorylation and dimerization of STAT3 (Fig. 4G, H), whereas overexpression of SNX3 by infecting with Ad-SNX3 had the opposite effects (Supplementary Fig. S10C–E). Collectively, these results suggest that SNX3–retromer serves as a platform for the assembly of gp130/JAK2/STAT3 complexes and the subsequent phosphorylation of STAT3 in ISO-induced cardiac hypertrophy model in vitro.

SNX3–retromer promoted the nuclear localization of STAT3

After treatment with stimuli of cardiac hypertrophy, cytoplasmic STAT3 shuttles to the nucleus (Supplementary Figs. S12A and S13), where STAT3 orchastreates hypertrophy-related target gene expression (such as *Anf, c-fos, c-myc, aGT*) [4, 35, 36]. Given that the SNX3–retromer complex plays a vital role in sorting cargoes from endosomes
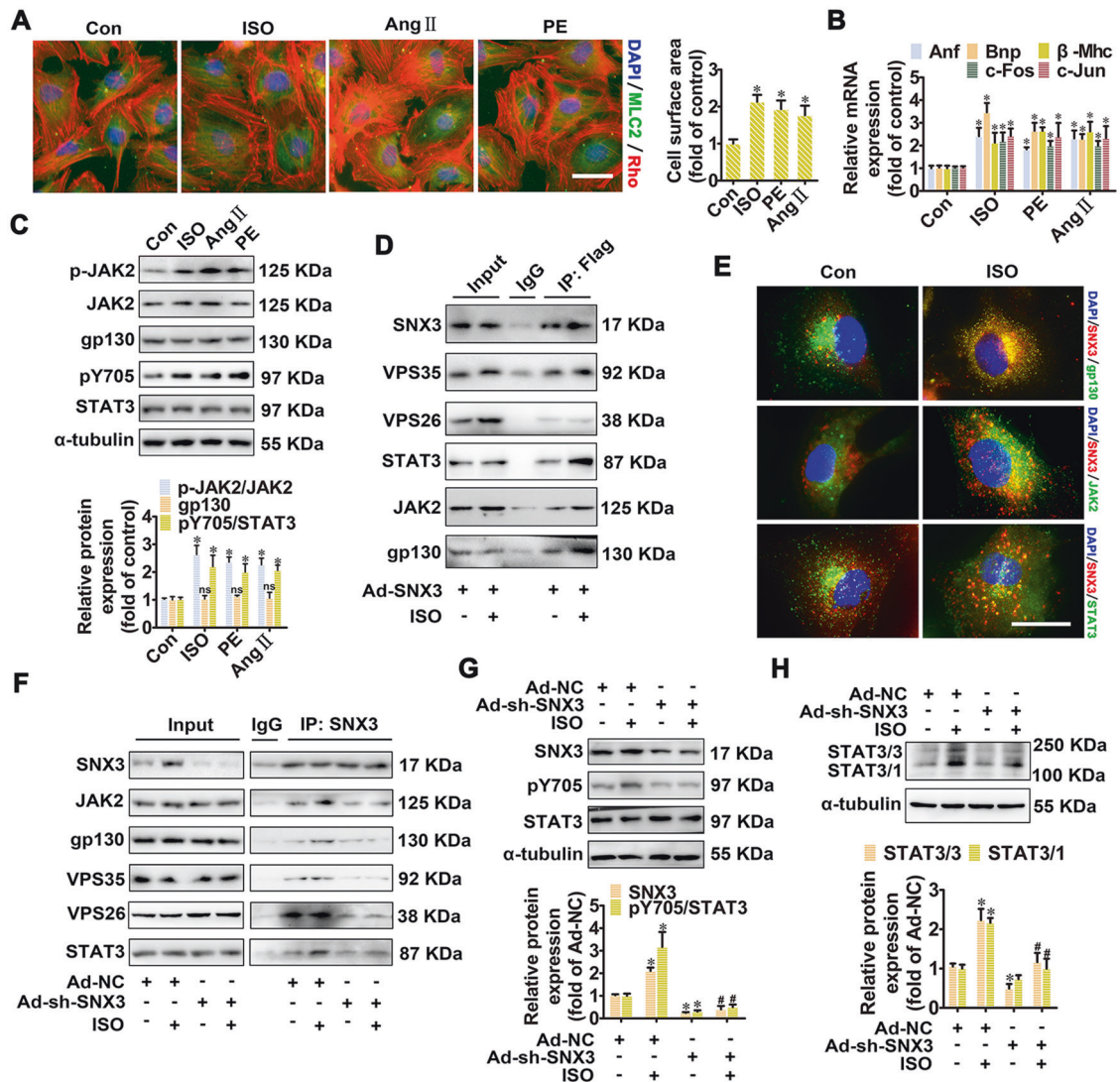
Fig. 4 SNX3–retromer acted as a platform for STAT3 activation in NRCMs. NRCMs were treated with three hypertrophic stimulants, including ISO (10 µmol/L), Ang II (1 µmol/L), and PE (100 µmol/L), respectively, for the times indicated. **A** The cell surface area was measured by staining with anti-MLC2 antibody (green) and rhodamine-phalloidin (red) (Scale bar: 25 µm). **B** The mRNA levels of *Anf*, *Bnp*, *β-Mhc*, *c-Fos*, and *c-Jun* were determined by qPCR. **C** Western blot analysis was performed to detect the phosphorylated JAK2 (at tyrosine 1007 and 1008, p-JAK2) and STAT3 (at tyrosine 705, pY705), as well as the protein expression of JAK2, gp130 and STAT3. **D** NRCMs infected with Ad-SNX3 (Flag-tagged) were treated with ISO for 1 h and were precipitated by anti-Flag antibody, followed by co-IP assays. **E** The intracellular co-localization of SNX3 and gp130, JAK2, STAT3 in ISO-treated NRCMs was determined using confocal microscopy (Scale bar: 25 µm). NRCMs were infected with Ad-sh-SNX3 followed by incubation with ISO (10 µmol/L for 1 h), were precipitated by anti-SNX3 in co-IP assays (**F**), were detected the phosphorylated STAT3 (pY705), the protein expression of SNX3 and STAT3 (**G**), and were examined the protein expression of STAT3/3 homodimer or STAT3/1 heterodimer (**H**). Representative images of five independent experiments were presented. The data were shown as the means ± SEM. *$P < 0.05$ vs. control or Ad-NC group, #$P < 0.05$ vs. Ad-NC + ISO group, $n = 5$. Ang II, angiotensin II; co-IP, co-immunoprecipitation, IF immunofluorescence, ISO isoproterenol, MLC2 myosin light chain 2, NC negative control, NRCMs neonatal rat cardiomyocytes, PE phenylephrine, qPCR quantitative polymerase chain reaction, 1h, 1 h. See also Supplementary Figs. S10 and S11A.

to the intracellular trafficking [6], we examined the effects of the SNX3–retromer on the subcellular distribution of STAT3 in the process of cardiac hypertrophy. NRCMs were treated with ISO, AngII, or PE, or were infected with Ad-SNX3 or Ad-sh-SNX3 before ISO treatment. The nuclear and cyto-plasmic proteins were extracted from NRCMs, and were detected by western blot analysis. The results showed that

transient nuclear import of STAT3, SNX3, VPS35, and VPS26, after treatment with hypertrophic stimuli for 1 h (Supplementary Fig. S12A). By contrast, SNX3 silencing reversed ISO-induced nuclear import of STAT3 using IF and western blot analysis (Fig. 5A, B). Similarly, the ISO-induced increase of transcriptional activity and target gene expression of STAT3 was inhibited by SNX3 knockdown in vitro
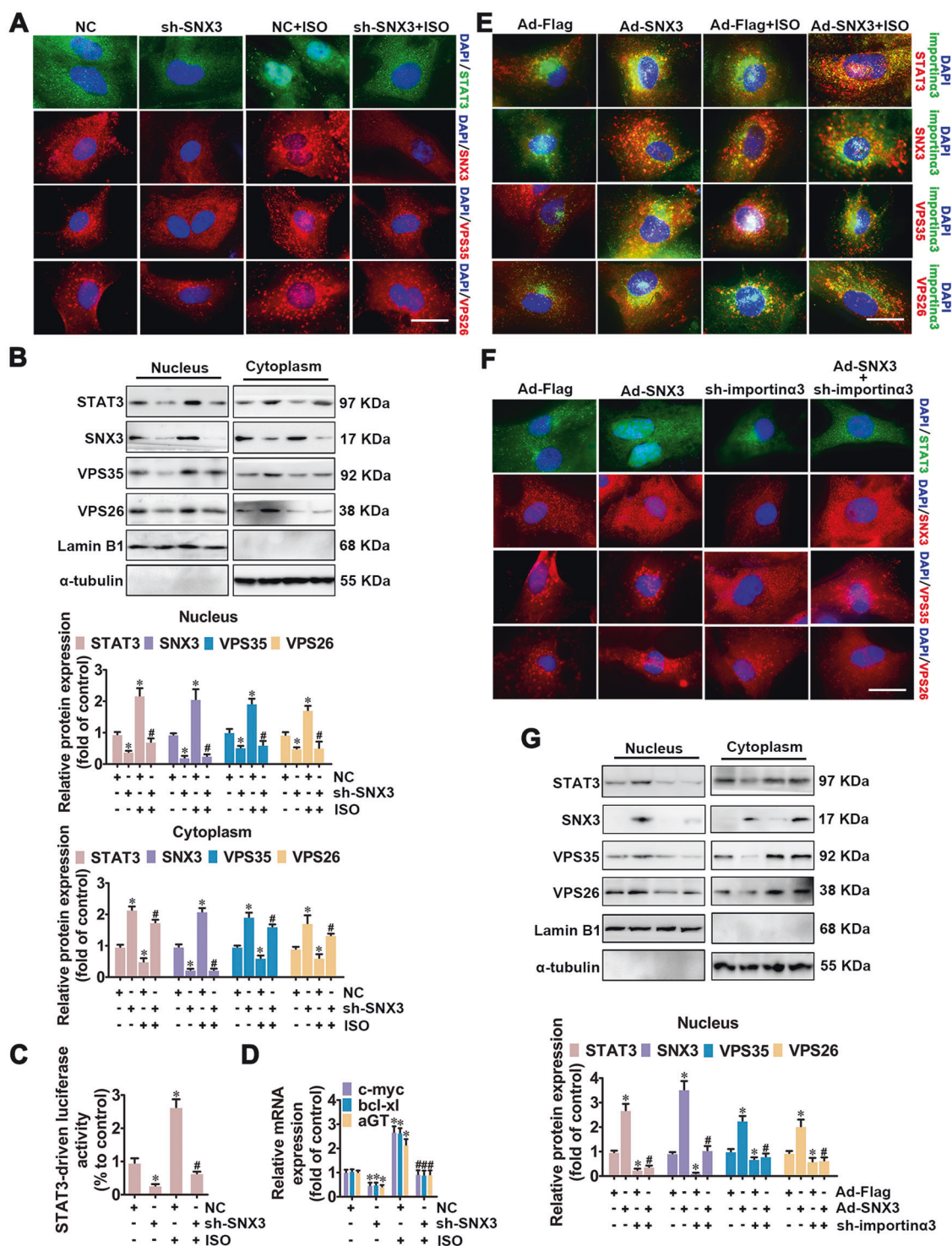
Fig. 5 SNX3–retromer promoted the nuclear localization of STAT3 in NRCMs. NRCMs were infected with Ad-sh-SNX3 or Ad-SNX3 before ISO treatment for 1 h. Besides, another group of NRCMs was infected with Ad-SNX3 followed by transfection with shRNAs of importin α3. **A**, **E**, and **F** IF assay was performed to detect the subcellular distribution of STAT3, SNX3, VPS35, and VPS26. Representative images of five independent experiments were presented. **B** and **G** The nuclear and cytoplasmic proteins were extracted from NRCMs, and were detected by western blot analysis. The results were normalized to those of α-tubulin/Lamin B1. **C** Luciferase reporter gene assays showed the transcriptional activity of STAT3. **D** The mRNA levels of the target genes of STAT3 (*c-myc*, *bcl-xl*, and *aGT*) were confirmed by qPCR. The data were shown as the means ± SEM. *$P < 0.05$ vs. NC or Ad-Flag group, #$P < 0.05$ vs. Ad-sh-SNX3 or Ad-SNX3 group, $n = 5$. IF immunofluorescence, ISO isoproterenol, NC negative control, NRCMs neonatal rat cardiomyocytes, qPCR quantitative polymerase chain reaction. See also Supplementary Figs. S11–S16.

(Fig. 5C, D) or by SNX3 knockout in vivo (Supplementary Fig. S14). JAK2 knockdown reversed overexpressed SNX3-induced nuclear import of STAT3 (Supplementary Fig. S11C). Knockdown of retromer components VPS35 attenuated the effects of SNX3 overexpression on STAT3 nuclear localization (Supplementary Fig. S15B). These results suggest that JAK2 was involved in SNX3–retromer-mediated STAT3 nuclear localization.

Previous studies have shown that importin α3, a nuclear importing factor, is responsible for STAT3 nuclear import induced by hormones or intracellular tyrosine kinases [21, 22]. The endogenous importin α3 was knocked down using the appropriate shRNA (Supplementary Fig. S12B, C). By IF staining, we observed that Ad-SNX3 treatment significantly increased ISO-induced interaction of importin α3 and STAT3–SNX3-retromer complexes (Fig. 5E). However, importin α3 knockdown attenuated Ad-SNX3-triggered the nuclear importing of STAT3 and SNX3-retromer (Fig. 5F, G, Supplementary Fig. S12D), suggesting that SNX3-retromer promoted the importin α3-mediated nuclear localization of STAT3 in cardiomyocytes.

Involvement of STAT3 in SNX3-mediated cardiomyocyte hypertrophy

We then asked whether SNX3 induces cardiomyocyte hypertrophy through STAT3 activation. Knockdown of SNX3 significantly suppressed the hypertrophic growth of cardiomyocytes induced by ISO, which was inhibited by STAT3 overexpression (Fig. 6A, B, Supplementary Fig. S17C and D). Conversely, Ad-SNX3 led to increased hypertrophic responses, which were partly inhibited by stattic (an inhibitor of STAT3) or STAT3 knockdown, implying that STAT3 was involved in SNX3-mediated cardiomyocyte hypertrophy (Fig. 6A, B, Supplementary Fig. S17C, D). Knockdown of retromer components VPS35 significantly suppressed the hypertrophic responses induced by Ad-SNX3 (Supplementary Fig. S15C, D). Similarly, SNX3 overexpression led to increased hypertrophic responses, which were obviously inhibited by JAK2 knockdown (Supplementary Fig. S11D, E). These data pinpoint that JAK2/STAT3 was involved in SNX3-retromer-mediated cardiac hypertrophy.

To further confirm the role of STAT3 in SNX3-induced cardiac injury in vivo, Snx3-cTg mice were treated with stattic (40 mg/kg/d, i.p.) or an equal volume of vehicle for 2 weeks. The phosphorylation level of STAT3 at the tyrosine 705 (pY705) was significantly inhibited by stattic, suggesting that the activation STAT3 was inhibited by stattic (Fig. 6D, E). After treatment with stattic, N-Tg mice showed no noticeable changes in cardiomyocytes (Fig. 6F–J, Supplementary Fig. S18A–M). However, the degree of cardiac hypertrophy (determined by gross observation of heart morphology, hypertrophic biomarkers, HW/TL ratio, WGA staining, and HE staining) of Snx3-cTg mice was significantly alleviated in stattic treatment group compared with that in the vehicle-treated group (Fig. 6F, H, Supplementary Fig. S18A, B, D). Besides, Snx3-cTg mice showed increased cardiomyocyte interstitial fibrosis (determined by PSR staining and masson staining), while that effect was widely suppressed upon stattic treatment (Fig. 6G, Supplementary Fig. S18C). The echocardiography data showed that Snx3-cTg reduced EF, FS, CO, LVV, LVID, and SV, increased LVPW, LVM, and IVS, which could be antagonized by stattic in different degrees (Fig. 6J, Supplementary Fig. S18E–L).

These results suggest that STAT3 was involved in SNX3 overexpression-induced cardiomyocyte hypertrophy in vivo and in vitro.

Discussion

SNX3 plays a crucial role in the pathogenesis of diverse diseases, including Parkinson's disease [17], Alzheimer's disease [37], and autosomal dominant polycystic kidney disease [15]. However, it remains unknown whether SNX3 plays a role in cardiac diseases. In this study, we observed that SNX3 expression was increased in end-stage failing human hearts and cardiac tissues from a mouse models of ISO-induced cardiac injury. In addition to ISO, two other classical neurohumoral stimuli (AngII and PE) can also increase the mRNA and protein levels of SNX3 in vitro. These findings indicate that SNX3 is a common mediator of neurohumoral stimulation-induced pro-hypertrophic signaling.

By using gain-of-function and loss-of-function experiments in vivo, we revealed a novel role of SNX3 in the development of cardiac hypertrophy and HF. This was evidenced by the fact that cardiac-specific Snx3-cKO protected mice against ISO-induced cardiac hypertrophy, conversely, Snx3-cTg mice were hypersensitive to ISO-induced cardiac hypertrophy and aggravated cardiac injury with advancing age.

It has been reported that the SNXs family affects a wide range of biological processes by regulating the intracellular trafficking of diverse signaling proteins [10–13, 38]. For instance, deficiency of SNX10 prevents inflammation and bone erosion in rheumatoid mouse arthritis through promoting NFATc1 degradation; [10] SNX13 profoundly affects cardiac performance through the SNX13–PXA–ARC–caspase signaling pathway; [11] Deletion of SNX27 reverses epithelial–mesenchymal transition in highly aggressive breast cancer cells [13]; SNX27 serves as an essential adaptor protein, mediates beta 2ARs to the retromer tubule and endosome-to-PM trafficking [38]. However, the effect of SNX3 on the intracellular transportation of cargo proteins, which is tightly

It was previously believed that retromer (VPS26–VPS35–VPS29 heterotrimers) act as the cargo-sorting complex [39, 40]. Recent studies have shown that SNX proteins are indispensable for cargo recognition, select, and binding [6, 41]. A T-shaped architecture of SNX3-retromer was identified, and this complex comprised SNX3, VPS26, and VPS35 [6]. SNX3–retromer complex play the central role in recycling various proteins (such as Wntless, transferrin receptor, and Fet3-Ftr1) from the endosomes to TGN or PM [14, 17, 37, 42–46]. SNX3–retromer mediate Wntless sorting and Wnt secretion [14, 42–44], which mediates cellular

associated with cardiovascular diseases, has not been evaluated yet. Considering that SNX3-retromer was found in the nucleus of hypertrophic cardiomyocytes in this study, IP–MS was performed to identify the possible nuclear proteins that might bind to SNX3. According to our results, we mainly focus on the specific role of SNX3–STAT3 interaction in cardiomyocytes. SNX3 was required for STAT3 activation, inhibition of STAT3 could reduce the detrimental role of overexpressed SNX3 in cardiomyocytes and *Snx3-cTg* mice. Of course, in addition to STAT3, there must be other target proteins of SNX3-retromer, which is also the focus of our future work.

Fig. 6 STAT3 was involved in SNX3-mediated cardiomyocyte hypertrophy in NRCMs and in *Snx3-cTg* mice. NRCMs were divided into four groups: (1) infected with Ad-sh-SNX3 before ISO treatment; (2) infected with Ad-SNX3 with or without stattic (5 μmol/L, 24 h); (3) transfected with si-STAT3 before infection of Ad-SNX3; (4) infected with Ad-STAT3 before transfection of Ad-sh-SNX3 in ISO-treated NRCMs. **A** The cell surface area was measured by staining with anti-MLC2 (green) and rhodamine-phalloidin (red) (Scale bar: 25 μm). **B** The mRNA expression of *Anf*, *Bnp*, *β-Mhc*, and *Snx*3 were measured by qPCR. Additionally, male *Snx3-cTg* mice (10-weeks-old) were administrated with stattic (40 mg/kg/d, i.p.) or an equal volume of vehicle for 2 weeks. **C–E** The protein expression of SNX3 and the phosphorylated STAT3 (pY705) were measured by IF (Scale bar: 100 μm) and western blot analysis. **F** and **G** HE staining (Scale bar: 100 μm) and PSR staining (Scale bar: 100 μm)-stained cross-sections of heart tissues were shown. **H** The HW/TL ratio was calculated. **I** The representative echocardiographic graphs was presented. **J** The echocardiographic parameter EF was measured. Representative images of five independent experiments were presented. The data were presented as the means ± SEM. *$P < 0.05$ vs. control, Ad-Flag, Ad-NC or *N-Tg* + Saline, group, #$P < 0.05$ vs. ISO, Ad-SNX3 or *Snx3-cTg* + Saline group, &$P < 0.05$ vs. Ad-sh-SNX3 or Ad-SNX3 group, $n = 5$ for cell test. $n = 12$ per *N-Tg* (12w) + Saline group, $n = 11$ per *Snx3-cTg* (12w) + Saline group, $n = 12$ per *N-Tg* (12w) + Stattic group, $n = 12$ per *Snx3-cTg* (12w) + Stattic group. EF ejection fraction, HE hematoxylin–eosin, HW/TL the heart weight to the tibia length ratio, IF immunofluorescence, i.p. intraperitoneally, ISO isoproterenol, MLC2 myosin light chain 2, NC negative control, NRCMs neonatal rat cardiomyocytes, ns no statistical difference, *N-Tg* non-transgenic, PSR picric sirius red, qPCR quantitative polymerase chain reaction, *Snx3-cTg* cardiac-specific *Snx3* transgenic, 1h 1 h. See also Supplementary Figs. S11, S15, S17–S19.

crosstalk to regulate glucose metabolism and cardiac homeostasis [47, 48]. SNX3 regulates the recycling of transferrin receptors and iron assimilation [37], which regulates cellular iron homeostasis in cardiomyocytes [49]. SNX3–retromer mediate retrograde recycling of iron transporters in *S. cerevisiae* and *C. elegans* models of Parkinson's disease [17, 37]. In iron-starved cells, Fet3-Ftr1 is sorted by SNX3/Grd19 and retromer into a recycling pathway that delivers it back to the PM [45, 46]. In this study, we identified STAT3 as a new interacting partner of the SNX3–retromer complex mainly in EE in cardiomyocytes.

STAT3 activity is tightly regulated for proper physiological processes, and its aberrant and persistent activation will result in pathological cardiac hypertrophy [4, 18]. Over-activation of STAT3 could be mainly attributed to either the stimulation of STAT3 activators (such as ISO and IL-6) or the aberrantly activated upstream tyrosine kinases (such as JAK2 and EGFR) [18–20]. The present work suggests that SNX3–retromer acts as an essential platform for the assembly of gp130/JAK2/STAT3 complexes induced by ISO, and subsequent phosphorylation of STAT3 by direct combining at EE.

To date, the main research of SNXs-mediated intracellular transportation is focused on the subcellular trafficking from the endosomes to TGN or PM [6]. It is rarely reported that the nuclear transport of intracellular proteins mediated by SNXs, except that SNX11 is required for the translocation of factor II receptor-like 1 (F2rl1) from the PM to the cell nucleus in retinal ganglion cells [7]. We report that the SNX3–retromer complex was transiently imported into the nucleus after hypertrophic stimuli, and promoted importin α3-dependent nuclear translocation of STAT3 in the cardiac hypertrophy model.

Considering that isolated cardiomyocytes in vitro could mainly simulate compensated cardiac hypertrophy, but could not simulate the stage of decompensated cardiac hypertrophy or HF, this may be the reason why the change of subcellular localization of SNX3 was not very consistent in vivo and in vitro. We speculate that SNX3 protein is increased in both cytoplasm and nucleus with the continuous stimulation of cardiac hypertrophy stimulant, the nuclear and cytoplasmic SNX3 proteins collaborate to play a role in the process of HF.

According to our work, it is plausible that SNX3–retromer promotes both STAT3 activation and nuclear translocation. The detailed mechanism whereby the complex is recruited to membrane receptor to be activated and subsequently directed to nuclear after activation is not clear yet. There may be another protein or posttranslational modification that determines the fate of the complex for intracellular trafficking.

In conclusion, the present study demonstrates that SNX3–retromer plays a critical role in cardiac function and suggests that SNX3 could be exploited as a potential new therapeutic target for cardiac hypertrophy and HF.

Materials and methods

Human heart samples

The study conforms to the principles that govern the use of human tissues outlined in the Declaration of Helsinki. Approval was obtained from the human ethics committee of First Affiliated Hospital of Sun Yat-sen University. All patients or the family of prospective heart donors gave written informed consent prior to participation. Failing human heart samples were collected from 9 patients undergoing heart transplantation because of end-stage HF (Table S1). Three non-failing control heart samples were obtained from prospective multi-organ donors, which did not exhibit cardiovascular pathology but were unable to be transplanted due to technical reasons. Tissue samples were collected at the time of explantation and rapidly frozen in liquid nitrogen or fixed with 4% paraformaldehyde.

Animal studies

Snx3-floxed mice were constructed in the Shanghai Model Organisms Center by CRISPR/Cas9 technology. Briefly,

the donor vector containing four guide RNAs and Cas9 mRNA targeting *Snx*3 introns 2 and 3 (Table S2) was microinjected into C57BL/6 mouse fertilized eggs. The positive founder mice were backcrossed with wild-type C57BL/6 mice to obtain heterozygous *Snx*3$^{flox/+}$ mice with germline transmission. *Snx*3$^{flox/+}$ mice were self-crossed to generate homozygous *Snx*3$^{flox/flox}$ mice. *Snx*3$^{flox/flox}$ mice were crossed with C57BL/6J-*Myh6*$^{em1(IRES-Cre)Smoc}$ mice (Shanghai Model Organisms Center, Stock No. NM-KI-00083. MGI ID: 97255) to generate *Myh6-Cre*$^+$; *Snx*3$^{flox/flox}$ mice, i.e. cardiac-specific *Snx3-cKO* mice.

Snx3 transgenic mice were constructed in the Shanghai Model Organisms Center using standard methods. Briefly, the Piggybac vector harboring mouse SNX3 cDNA was microinjected into the fertilized egg of the C57BL/6 mouse, and the transgenic founder mice were obtained. Three generations of a backcross between each *Snx3* transgenic mice and wild-type (C57BL/6) mice were adopted to breed two independent *Snx3* transgenic lines. The two transgenic lines were, respectively, crossed with B6.FVB-Tg(Myh6-Cre)2182Mds/J mice (Jackson Laboratory (Bar Harbor, ME), Stock No. 011038. MGI ID: 2386742) to generate cardiac-specific over-expressed *Snx*3 (*Snx3-cTg*) mice.

The mice were genotyped by PCR and further confirmed by western blot analysis (Tables S3–S5). All animal protocols were conducted under the institutional guidelines of the Animal Care and Use Committee and were approved by the Research Ethics Committee, Sun Yat-sen University. Experimental animals were housed, bred, and maintained in the specific pathogen-free (SPF) facility of the Experimental Animal Center of Sun Yat-sen University. As we previously described [30], the transthoracic 2D-guided M-mode echocardiography (such as heart function and global cardiac volumes) was assessed using a Technos MPX ultrasound system (ESAOTE, SpAESAOTE SpA, Italy) equipped with a 40-MHz scan probe by an investigator who was blinded to the specific group assignment. The Vevo 2100 imaging software was used for measurements and calculations. Then, the treated mice were sacrificed, and hearts were rapidly sampled for further experiments.

Bioluminescence imaging

XenoLight^{TM} D-luciferin potassium salt (PerkinElmer, P/N 122799) was diluted in sterile PBS to 15 mg/mL and was, respectively, injected into the luciferase-labeled *Snx3-cTg* mice or *N-Tg* mice (150 mg/kg). A few minutes after injection, mice were anesthetized using 2% isoflurane inhalation (with a 2 L/min oxygen flow rate), and were placed inside the camera box of the IVIS Lumina XR small animal optical imaging system (PerkinElmer). The sequential images of the mice were run every 2 min.

Lumazone Version 2.0 software was used to analyze the intensity of the fluorescence (intensity/s) in mice [50].

Histological analysis

Myocardial tissue samples were fixed in 10% paraformaldehyde and embedded in paraffin for sectioning. Sections were stained with WGA, HE, Masson's, and PSR for histopathological examination under a light microscope.

For immunofluorescent (IF), paraffin sections of myocardial samples were treated with primary anti-SNX3 (Proteintech, #10772-1-AP) or anti-p-STAT3 (Y705, Cell Signaling Technology, CST, Beverly, MA, USA, #9145) overnight at 4 °C. Then, the samples were incubated with CoraLite488/594-conjugated anti-rabbit IgG (diluted 1:200, Proteintech, #SA00013-6 or #SA00013-8), were counterstained with 4′,6-diamidino-2-phenylindole (DAPI, CST, #4083). Fluorescence was captured by EVOS FL Auto (Life Technologies, Bothell, WA, USA).

Plasmid, recombinant adenoviral vectors, and recombinant protein

Vps26 (NM_001007740.1), *Vps35* (NM_001105718.2), *Snx3* (NM_001044283.1), and *Stat3* (NM_012747.2) were constructed by ligating respective full-length cDNA into pcDNA3.1 (+) with Flag or HA-tag. Similarly, short hairpin (sh) RNA targeting the rat's *importin α3* gene (also called as *Kpna3*, NM_001014792) (sh-importin α3), the rat's *Snx3* gene (sh-SNX3), and non-targeting control shRNA (sh-NC) sequences (Tables S6 and S7) were, respectively, subcloned into pcDNA3.1 (+) with Flag-tag.

Recombinant adenoviral vectors expressing rats *Snx3* cDNA (Ad-SNX3, with Flag-tag), rats STAT3 cDNA (Ad-STAT3, with HA-tag), sh-SNX3 sequence (Ad-sh-SNX3, with Flag-tag), and control vectors were generated by standard procedures. Briefly, the pAdTrack plasmids containing corresponding genes were linearized by using restriction endonuclease *PmeI*, and were transformed into *Escherichia coli* strain BJ5183 cells carrying the Ad-Easy-1 plasmid. The successful recombinant plasmids were digested with restriction endonuclease *PacI*, and were transfected into HEK293A cells to generate Ad-SNX3, Ad-STAT3, or Ad-sh-SNX3. The vectors were purified by plaque, cultured on a large scale, and purified by CsCl step-gradient and isopycnic-gradient centrifugation.

GST-STAT3, GST-SNX3, GST-VPS35, and GST-VPS26 protein (pGEX-4T-1 vector) were, respectively, expressed in *E. coli* BL21 (DE3) maintained in Luria-Bertani (LB) medium (including 50 µg/mL ampicillin) at 37 °C. By the addition of isopropyl-β-D-thiogalactopyranoside (IPTG, 0.5 mmol/L), protein expression was induced at 16 °C overnight to an OD600 value of 0.8. Cells were

re-suspended in 20 mmol/L Tris + 200 mmol/L NaCl + 1 mmol/L PMSF, were broken using ultrasonic instrument in ice, and were collected supernatant after centrifugation (12,000 rpm for 3 h at 4 °C). These recombinant protein were purified by GST-Sefinose Gravity Column, were enzyme digested at room temperature overnight. All purified protein were dissolved in sterile phosphate-buffered saline (PBS), their concentration were measured and stored at −80 °C.

LSPR assays

To examine the direct interaction between STAT3 and SNX3-retromer, LSPR assays were conducted on an OpenSPR system (Nicoya Lifesciences, Waterloo, Canada). Recombinant proteins STAT3 (117-770aa, 576-678aa), SNX3, and VPS35 served as the ligand and were, respectively, immobilized on a gold nanoparticle sensor chip via capture-coupling. Subsequently, the recombinant protein SNX3, VPS35, and VPS26 at different concentrations were sequentially injected into the chamber in running buffer (filtered PBS) with a constant flow rate of 20 µL/min, and were passed over the sensor (about 5 min) for the association of two protein. Following each recombinant protein injection (all concentrations were performed in triplicate), the chip was completely dissociated with the complex and regenerated by injecting hydrochloric acid (pH 2.0). As recommended by the manufacturer, the results were analyzed by Trace Drawer software (Ridgeview Instruments AB). The kinetic parameters, including the association constant (k_a), dissociation constant (k_d) and affinity (KD, KD = k_d/k_a), were calculated by a simple 1:1 dilution corrected model, which adjusted to the wavelength shifts consisting with the varied concentration of protein [51].

Proximity ligation assay

NRCMs cultured in coverslips were infected with Ad-SNX3 (Flag-tagged) and Ad-STAT3 (HA-tagged) before ISO (10 µM) treatment for 1 h. After treatment, cells were washed with filtered PBS for three times, fixed with 4% paraformaldehyde for 10 min, and permeabilized with 0.3% Triton X-100 for 5 min. After washing with filtered PBS, add blocking solution to each sample for 1 h at room temperature. NRCMs were stained with anti-Flag rabbit antibody and anti-HA mouse antibody in a humidity chamber overnight at 4 °C. Then, the PLA was performed according to the manufacturer instructions (Duolink™ In Situ Red Starter Kit Mouse/Rabbit (red), catalog #DUO92101, Sigma-Aldrich). The cells were incubated with the PLA probe solution (1 h, 37 °C), and were incubated with ligation–ligase solution (30 min, 37 °C) in a pre-heated

humidity chamber. After washing, coverslips were incubated with the amplification reaction mixture (100 min, 37 °C) in a pre-heated humidity chamber, washed, and counterstained with DAPI (blue). The images were observed by a confocal microscope (Zeiss, Germany) and analyzed by the Axiovision software (Zeiss). Each red dot represents the detection of protein–protein interactions (the distance between the two proteins is <40 nm) [52].

Primary culture of NRCMs

As reported before [30], NRCMs were isolated from the hearts of one to 3-day-old SD rats. Cardiomyocytes were plated into six-well microplates (Corning, USA) comprising Dulbecco's modified Eagle's medium (DMEM, Gibco, USA) supplemented with 10% newborn calf serum (NBCS) and 5-bromodeoxyuridine (Sigma, #B5002, 0.1 mmol/L), at a density of 1×10^6 cells/well.

Plasmid transfection and virus infections

NRCMs were transfected with sh-SNX3 plasmid (Table S6), sh-importin α3 (Table S7), si-STAT3 (Table S8), si-VPS35 (Table S9), or si-JAK2 (Table S10) together with lipofectamine 3000 reagent (Invitrogen, USA) in OptiMEM medium as per the manufacturer's instructions. The medium was changed to DMEM complete medium after 8–72 h of transfection. NRCMs were infected with recombinant adenoviruses (including Flag-tagged SNX3, Flag-tagged sh-SNX3, or HA-tagged STAT3) at a multiplicity of infection (MOI) of 20 particles per 5 cells. Western blot and/or Quantitative RT-PCR were performed to confirm the efficiency of overexpression or depletion [53].

Measurement of the cell surface area

NRCMs were seeded in 24-well microplates, fixed with paraformaldehyde (4%, Beyotime, #P0099) for 10 min at room temperature. After permeabilizing with Triton X-100 (0.3%, Beyotime, #P0096) and blocking with goat serum (Beyotime, #C0265), the cells were incubated with primary antibody myosin light chain 2 (MLC2, Proteintech, #10906-1-AP) overnight at 4 °C, treated with secondary antibody anti-alexa fluor 488 (Proteintech, #SA00013-6, for 2 h) and rhodamine-phalloidin (0.1%, Invitrogen #R415, for 30 min) at room temperature. After washing with filtered PBS, NRCMs were mounted by using DAPI (CST, #4083). The images were taken using the High Content Screening System (Thermo Fisher Scientific, USA), and the cell surface area from randomly selected fields (50 for each group) was analyzed by the built-in image analysis software [30, 53, 54].

J. Lu et al.

Isolation of EE by continuous density gradient centrifugation

The nuclear and cytoplasmic protein was successively extracted from NRCMs using a kit (SC-003, Inventbiotech, MN, USA). The postnuclear fraction was suspended in buffer, and was used as a continuous sucrose density gradient. After centrifugation ($210,000 \times g$ for 3 h at 4 °C), a milky band should be visible at each interface. 24 consecutive fractions were collected from each interface into tubes, and were subjected to western blot analysis for detection of protein EEA1, which is an early endosomal marker [55, 56].

Low temperature SDS–PAGE, Western blot and co-immunoprecipitation (co-IP) analysis

Low-temperature SDS–PAGE was conducted to investigate the homodimers (STAT3/STAT3) or heterodimer (STAT3/STAT1). In short, total protein from NRCMs were incubated in loading buffer (without 2-mercaptoethanol) for 5 min at 37 °C, were separated by 8% SDS–PAGE for 4–5 h at a constant current of 40 mA, and were transferred to a PVDF membranes (Millipore). The whole process of the experiment must be made under the low temperature. After blocking with 10% blocking buffer (Beyotime, #P0023B), the membranes were incubated with individual antibodies at 4 °C overnight [57].

Western blot analysis was performed as previously reported [53, 54]. Immunoblots were labeled with the following primary antibodies: primary antibodies against p-JAK2 (Y1007 and Y1008, rabbit, diluted 1:500, #3776), JAK2 (rabbit, diluted 1:1000, #3230), gp130 (rabbit, diluted 1:1000, #3732), p-STAT3 (Y705, rabbit, diluted 1:1000, #9145), STAT3 (rabbit, diluted 1:2000, #9139) were bought form CST. Primary antibodies against CHC (rabbit, diluted 1:1000), EEA1 (rabbit, diluted 1:1,000) and Rab5 (rabbit, diluted 1:1000) were purchased from CST (endosomal marker antibody sampler kit, #12666). SNX3 (rabbit, diluted 1:1000, #10772-1-AP), VPS26 (rabbit, diluted 1:800, #15915-1-AP) and VPS35 (rabbit, diluted 1:800, #10236-1-AP) were products of Proteintech. Primary antibodies against importin α3 (rabbit, diluted 1:1000, #I9783), HA (rabbit, diluted 1:5000, #H6908), and α-tubulin (mouse, diluted 1:5000, #T8203) were purchased from Sigma-Aldrich. Anti-Flag (mouse, diluted 1:5000, #PM185), anti-Lamin B1 (rabbit, diluted 1:1000, # PM064) were purchased from MBL. The enzyme horseradish peroxidase (HRP)-conjugated secondary antibodies (CST, #7074 and #7076) were applied to chemiluminescence detection and the protein band intensities were quantified by LabWorks software (Bio-Rad, USA).

For co-IP, anti-EEA1 (rabbit, diluted 1:50), anti-CHC (rabbit, diluted 1:50), anti-Rab5 (rabbit, diluted 1:20) were purchased from CST (endosomal marker antibody sampler kit, #12666), anti-VPS26 (rabbit, diluted 1:20, #15915-1-AP), and anti-VPS35 (rabbit, diluted 1:20, #10236-1-AP) were products of Proteintech. Anti-Flag (rabbit, diluted 1:50, #PM185) was purchased from MBL. Anti-HA (rabbit, diluted 1:50, #H6908) was purchased from Sigma-Aldrich. The rabbit normal IgG (#3900) and mouse normal IgG (#53484) were purchased from CST. NRCMs were harvested with IP lysis buffer (Beyotime, # P0013) supplemented with protease and phosphatase inhibitor cocktails (Bimake, #B14012 and #B15002). After clarification by centrifugation, 400–600 μg of total protein cell lysate were incubated with the indicated primary antibodies overnight at 4 °C, and were incubated with protein G-agarose beads (Pierce, Rockford, IL, USA) at 4 °C for 4 h. Normal IgG was served as an control. The immunoprecipitated proteins were detected by western blot.

IF assay

NRCMs were cultured in chamber slides (ThermoFisher Scientific). After treatment, cells were washed with filtered PBS for three times, fixed with 4% paraformaldehyde for 10 min, permeabilized with 0.3% Triton X-100 for 5 min and followed by blocking with goat serum for 1 h at room temperature. The cells were further treated with the following primary antibodies overnight at 4 °C: STAT3 (CST, #9139), SNX3 (Proteintech, #10772-1-AP), VPS35 (Proteintech, #10236-1-AP), VPS26 (Proteintech, #15915-1-AP), EEA1 (CST, #12666), Rab5 (CST, #12666), Rab7 (CST, #12666), CHC (CST, #12666), Lamp-2 (Proteintech, #66301-1-Ig), gp130 (CST, #3732), JAK2 (CST, #3230), and importin α3 (Sigma-Aldrich, #I9783). Fluorescence emitted by fluorescence-conjugated secondary antibodies (Proteintech, #SA00013-6 and #SA00013-8) at room temperature for 2 h. The slides were mounted with DAPI (CST, #4083) and were observed by a confocal microscope (Zeiss, Germany) or EVOS FL Auto (Life Technologies).

Total RNA isolation, cDNA synthesis, and real-time polymerase chain reaction (qPCR)

Total RNA was extracted from snap-frozen cardiac tissues or NRCMs by using Trizol reagent (Invitrogen, #15596026), and its concentration was measured with a Nanodrop 2000 (Thermo Fisher Scientific, USA). The RNA extract (1000 ng) was reversely transcribed to first strand cDNA using the One-step Reverse Transcription (RT) Kit (Thermo Fisher Scientific, USA). Quantitative SYBR Green-based PCR (TOYOBO, Janpan) was conducted on

SPRINGER NATURE

the iCycler iQ system (Bio-Rad, USA). GAPDH was used as reference gene. All PCR assays were performed in triplicate. Data were analyzed using the $2^{-\Delta\Delta CT}$ method. The oligonucleotide sequences are synthesized by Sangon (Shanghai, China), and listed in Table S11.

Dual-luciferase reporter gene assay

The conserved DNA-binding sequence of rats STAT3 (TTCCGGGAA) were subcloned into pGL3 Basic plasmid (Promega, #E1751) [58]. NRCMs were seeded at 5×10^4 cells per well into 96-well microplates, and were transiently co-transfected with the luciferase reporter (100 ng/well) and pRL-TK reporter constructs (Promega, E2241) at 20 ng/well. The total content of transfected DNA was normalized by empty vector. After the indicated treatments, the luciferase activity was determined by the dual-luciferase reporter assay system (Promega, #E1980) on a microplate reader (TECAN Infinite M1000).

Statistical analysis

Graph Pad Prism 6.0 (Graph Pad software) or SPSS Version 21 was used for statistical analysis. Normality of the obtained data was assessed using a Shapiro–Wilk test. When normality was confirmed, statistical differences among groups were analyzed using either Student's t test (for two groups) or one (or two)-way analysis of variance (ANOVA, for more than two groups). Otherwise, the non-parametric test Kruskal–Wallis test followed by the Dunn's post-hot test was used to correct for multiple comparisons. The Levene or Brown–Forsynth test was used to compare the variance between the two groups. In all cases, differences were considered statistically significant at a P value (two-sided) < 0.05.

Compliance with ethical standards

References

1. Brown DA, Perry JB, Allen ME, Sabbah HN, Stauffer BL, Shaikh SR, et al. Mitochondrial function as a therapeutic target in heart failure. Nat Rev Cardiol. 2017;14:238–50.
2. Roger VL, Go AS, Lloyd-Jones DM, Benjamin EJ, Berry JD, Borden WB, et al. Amer Heart Assoc Stat, S. Stroke Stat, Heart disease and stroke statistics-2012 update a report from the American Heart Association. Circulation. 2012;125:E2–E220.
3. Heineke J, Molkentin JD. Regulation of cardiac hypertrophy by intracellular signalling pathways. Nat Rev Mol Cell Biol. 2006;7:589–600.
4. Kunisada K, Negoro S, Tone E, Funamoto M, Osugi T, Yamada S, et al. Signal transducer and activator of transcription 3 in the heart transduces not only a hypertrophic signal but a protective signal against doxorubicin-induced cardiomyopathy. Proc Natl Acad Sci USA. 2000;97:315–9.
5. Kovtun O, Leneva N, Bykov YS, Ariotti N, Teasdale RD, Schaffer M, et al. Structure of the membrane-assembled retromer coat determined by cryo-electron tomography. Nature. 2018;561:561–4.
6. Lucas M, Gershlick DC, Vidaurrazaga A, Rojas AL, Bonifacino JS, Hierro A. Structural mechanism for cargo recognition by the retromer complex. Cell. 2016;167:1623–35.e14.
7. Joyal JS, Nim S, Zhu T, Sitaras N, Rivera JC, Shao Z, et al. Subcellular localization of coagulation factor II receptor-like 1 in neurons governs angiogenesis. Nat Med. 2014;20:1165–73.
8. Cullen PJ, Korswagen HC. Sorting nexins provide diversity for retromer-dependent trafficking events. Nat Cell Biol. 2011;14:29–37.
9. Cullen PJ. Endosomal sorting and signalling: an emerging role for sorting nexins. Nat Rev Mol Cell Biol. 2008;9:574–82.
10. Zhou C, You Y, Shen W, Zhu YZ, Peng J, Feng HT, et al. Deficiency of sorting nexin 10 prevents bone erosion in collagen-induced mouse arthritis through promoting NFATc1 degradation. Ann Rheum Dis. 2016;75:1211–8.
11. Li J, Li CM, Zhang DS, Shi D, Qi M, Feng J, et al. SNX13 reduction mediates heart failure through degradative sorting of apoptosis repressor with caspase recruitment domain. Nat Commun. 2014;5:5177.
12. Okada H, Zhang W, Peterhoff C, Hwang JC, Nixon RA, Ryu SH, et al. Proteomic identification of sorting nexin 6 as a negative regulator of BACE1-mediated APP processing. FASEB J. 2010;24:2783–94.
13. Zhang JL, Li K, Zhang YG, Lu R, Wu SP, Tang JR, et al. Deletion of sorting nexin 27 suppresses proliferation in highly aggressive

breast cancer MDA-MB-231 cells in vitro and in vivo. BMC Cancer. 2019;19:555.

14. McGough IJ, de Groot REA, Jellett AP, Betist MC, Varandas KC, Danson CM, et al. SNX3-retromer requires an evolutionary conserved MON2:DOPEY2:ATP9A complex to mediate Wntless sorting and Wnt secretion. Nat Commun. 2018;9:3737.

15. Feng S, Streets AJ, Nesin V, Tran U, Nie H, Onopiuk M, et al. The sorting nexin 3 retromer pathway regulates the cell surface localization and activity of a Wnt-activated polycystin channel complex. J Am Soc Nephrol. 2017;28:2973–84.

16. Cui Y, Carosi JM, Yang Z, Ariotti N, Kerr MC, Parton RG, et al. Retromer has a selective function in cargo sorting via endosome transport carriers. J Cell Biol. 2019;218:615–31.

17. Patel D, Xu C, Nagarajan S, Liu Z, Hemphill WO, Shi R, et al. Alpha-synuclein inhibits Snx3-retromer-mediated retrograde recycling of iron transporters in S. cerevisiae and C. elegans models of Parkinson's disease. Hum Mol Genet. 2018;27:1514–32.

18. Wang L, Li Z, Tan Y, Li Q, Yang H, Wang P, et al. PARP1 interacts with STAT3 and retains active phosphorylated-STAT3 in nucleus during pathological myocardial hypertrophy. Mol Cell Endocrinol. 2018;474:137–50.

19. Zhang W, Qu X, Chen B, Snyder M, Wang M, Li B, et al. Critical roles of STAT3 in beta-adrenergic functions in the heart. Circulation. 2016;133:48–61.

20. Zhang HX, Xu ZS, Lin H, Li M, Xia T, Cui K, et al. TRIM27 mediates STAT3 activation at retromer-positive structures to promote colitis and colitis-associated carcinogenesis. Nat Commun. 2018;9:3441.

21. Liu L, McBride KM, Reich NC. STAT3 nuclear import is independent of tyrosine phosphorylation and mediated by importin-alpha 3. Proc Natl Acad Sci USA. 2005;102:8150–5.

22. Reich NC, Liu L. Tracking STAT nuclear traffic. Nat Rev Immunol. 2006;6:602–12.

23. Ohara R, Fujita Y, Hata K, Nakagawa M, Yamashita T. Axotomy induces axonogenesis in hippocampal neurons through STAT3. Cell Death Dis. 2011;2:e175.

24. Ben-Yaakov K, Dagan SY, Segal-Ruder Y, Shalem O, Vuppalanchi D, Willis DE, et al. Axonal transcription factors signal retrogradely in lesioned peripheral nerve. EMBO J. 2012;31:1350–63.

25. Di Liberto V, Cavalli V. Ready, STAT, go: transcription factors on the move. EMBO J. 2012;31:1331–3.

26. Mukhopadhyay S, Shah M, Xu F, Patel K, Tuder RM, Sehgal PB. Cytoplasmic provenance of STAT3 and PY-STAT3 in the endolysosomal compartments in pulmonary arterial endothelial and smooth muscle cells: implications in pulmonary arterial hypertension. Am J Physiol Lung Cell Mol Physiol. 2008;294:L449–68.

27. Bild AH, Turkson J, Jove R. Cytoplasmic transport of Stat3 by receptor-mediated endocytosis. EMBO J. 2002;21:3255–63.

28. German CL, Sauer BM, Howe CL. The STAT3 beacon: IL-6 recurrently activates STAT 3 from endosomal structures. Exp Cell Res. 2011;317:1955–69.

29. Kermorgant S, Parker PJ. Receptor trafficking controls weak signal delivery: a strategy used by c-Met for STAT3 nuclear accumulation. J Cell Biol. 2008;182:855–63.

30. Li J, Huang J, Lu J, Guo Z, Li Z, Gao H, et al. Sirtuin 1 represses PKC-zeta activity through regulating interplay of acetylation and phosphorylation in cardiac hypertrophy. Br J Pharmacol. 2019;176:416–35.

31. Hashimoto T, Kim GE, Tunin RS, Adesiyun T, Hsu S, Nakagawa R, et al. Acute enhancement of cardiac function by phosphodiesterase type 1 inhibition: translational study in the dog and rabbit. Circulation. 2018;138:1974–87.

32. Zhang N, Zhang Y, Qian H, Wu S, Cao L, Sun Y. Selective targeting of ubiquitination and degradation of PARP1 by E3 ubiquitin ligase WWP2 regulates isoproterenol-induced cardiac remodeling. Cell Death Differ. 2020;27:2605–19.

33. Li Y, Lv Z, He L, Huang X, Zhang S, Zhao H, et al. Genetic tracing identifies early segregation of the cardiomyocyte and nonmyocyte lineages. Circ Res. 2019;125:343–55.

34. Agah R, Frenkel PA, French BA, Michael LH, Overbeek PA, Schneider MD. Gene recombination in postmitotic cells. Targeted expression of Cre recombinase provokes cardiac-restricted, site-specific rearrangement in adult ventricular muscle in vivo. J Clin Investig. 1997;100:169–79.

35. Kunisada K, Tone E, Fujio Y, Matsui H, Yamauchi-Takihara K, Kishimoto T. Activation of gp130 transduces hypertrophic signals via STAT3 in cardiac myocytes. Circulation. 1998;98:346–52.

36. Frias MA, Rebsamen MC, Gerber-Wicht C, Lang U. Prostaglandin E2 activates Stat3 in neonatal rat ventricular cardiomyocytes: a role in cardiac hypertrophy. Cardiovasc Res. 2007;73:57–65.

37. Chen C, Garcia-Santos D, Ishikawa Y, Seguin A, Li L, Fegan KH, et al. Snx3 regulates recycling of the transferrin receptor and iron assimilation. Cell Metab. 2013;17:343–52.

38. Temkin P, Lauffer B, Jager S, Cimermancic P, Krogan NJ, von Zastrow M. SNX27 mediates retromer tubule entry and endosome-to-plasma membrane trafficking of signalling receptors. Nat Cell Biol. 2011;13:715–21.

39. Nothwehr SF, Bruinsma P, Strawn LA. Distinct domains within Vps35p mediate the retrieval of two different cargo proteins from the yeast prevacuolar/endosomal compartment. Mol Biol Cell. 1999;10:875–90.

40. Seaman MN, McCaffery JM, Emr SD. A membrane coat complex essential for endosome-to-Golgi retrograde transport in yeast. J Cell Biol. 1998;142:665–81.

41. Gallon M, Clairfeuille T, Steinberg F, Mas C, Ghai R, Sessions RB, et al. A unique PDZ domain and arrestin-like fold interaction reveals mechanistic details of endocytic recycling by SNX27-retromer. Proc Natl Acad Sci USA. 2014;111:E3604–13.

42. Zhang P, Wu YH, Belenkaya TY, Lin XH. SNX3 controls Wingless/Wnt secretion through regulating retromer-dependent recycling of Wntless. Cell Res. 2011;21:1677–90.

43. Lorenowicz MJ, Macurkova M, Middelkoop TC, de Groot R, Betist MC, Korswagen HC. Inhibition of late endosomal maturation restores Wnt secretion in Caenorhabditis elegans vps-29 retromer mutants. Cell Signal. 2014;26:19–31.

44. Harterink M, Port F, Lorenowicz MJ, McGough IJ, Silhankova M, Betist MC, et al. A SNX3-dependent retromer pathway mediates retrograde transport of the Wnt sorting receptor Wntless and is required for Wnt secretion. Nat Cell Biol. 2011;13:914–23.

45. Strochlic TI, Schmiedekamp BC, Lee J, Katzmann DJ, Burd CG. Opposing activities of the Snx3-retromer complex and ESCRT proteins mediate regulated cargo sorting at a common endosome. Mol Biol Cell. 2008;19:4694–706.

46. Strochlic TI, Setty TG, Sitaram A, Burd CG. Grd19/Snx3p functions as a cargo-specic adapter for retromer-dependent endocytic recycling. J Cell Biol. 2007;177:115–25.

47. Xu WJ, Barrientos T, Mao L, Rockman HA, Sauve AA, Andrews NC. Lethal cardiomyopathy in mice lacking transferrin receptor in the heart. Cell Rep. 2015;13:533–45.

48. Gross JC, Zelarayán LC. The mingle-mangle of Wnt signaling and extracellular vesicles: functional implications for heart research. Front Cardiovasc Med. 2018;5:10.

49. Lakhal-Littleton S. Mechanisms of cardiac iron homeostasis and their importance to heart function. Free Radic Biol Med. 2019;133:234–37.

50. Yin CR, Zhang T, Qu XY, Zhang YG, Putatunda R, Xiao X, et al. In vivo excision of HIV-1 provirus by saCas9 and multiplex single-guide RNAs in animal models. Mol Ther. 2017;25:1168–86.

51. Tao Z, Yang H, Shi Q, Fan Q, Wan L, Lu X. Targeted delivery to tumor-associated pericytes via an affibody with high affinity for

PDGFRbeta enhances the in vivo antitumor effects of human TRAIL. Theranostics. 2017;7:2261–76.

52. Cottrell GS, Soubrane CH, Hounshell JA, Lin H, Owenson V, Rigby M, et al. CACHD1 is an α2δ-Like protein that modulates Ca(V)3 voltage-gated calcium channel activity. J Neurosci. 2018;38:9186–201.

53. Lu J, Zhang RW, Hong HQ, Yang ZL, Sun DP, Sun SY, et al. The poly(ADP-ribosyl)ation of FoxO3 mediated by PARP1 participates in isoproterenol-induced cardiac hypertrophy. Biochim Biophys Acta. 2016;1863:3027–39.

54. Lu J, Sun DP, Liu ZP, Li M, Hong HQ, Liu C, et al. SIRT6 suppresses isoproterenol-induced cardiac hypertrophy through activation of autophagy. Transl Res. 2016;172: 96–112.

55. de Araujo ME, Lamberti G, Huber LA. Isolation of early and late endosomes by density gradient centrifugation. Cold Spring Harb Protoc. 2015;2015:1013–6.

56. Nakatsuka S, Hayashi M, Muroyama A, Otsuka M, Kozaki S, Yamada H, et al. D-aspartate is stored in secretory granules and released through a Ca^{2+}-dependent pathway in a subset of rat pheochromocytoma PC12 cells. J Biol Chem. 2001;276:26589–96.

57. Luo WW, Wang Y, Yang HW, Dai CM, Hong HL, Li JY, et al. Heme oxygenase-1 ameliorates oxidative stress-induced endothelial senescence via regulating endothelial nitric oxide synthase activation and coupling. Aging. 2018;10:1722–44.

58. Horvath CM, Wen Z, Darnell JEA. STAT protein domain that determines DNA sequence recognition suggests a novel DNA-binding domain. Genes Dev. 1995;9:984–94.